POLYMORPHISM IN LATTICE MODELS

MARCIA M. SZORTYKA,[1] MAURICIO GIRARDI,[2] CARLOS E. FIORE,[3] VERA B. HENRIQUES,[4] and MARCIA C. BARBOSA[5]

[1]*Departamento de Física, Universidade Federal de Santa Catarina, Caixa Postal 476, 88010-970, Florianópolis, SC, Brazil*
[2]*Universidade Federal de Santa Catarina, 88900-000, Araranguá, SC, Brazil*
[3]*Departamento de Física, Universidade Federal do Paraná, Caixa Postal 19044, 81531 Curitiba, PR, Brazil*
[4]*Instituto de Física, Universidade de São Paulo, Caixa Postal 66318, 05315970, São Paulo, SP, Brazil*
[5]*Instituto de Física, Universidade Federal do Rio Grande do Sul, Caixa Postal 15051, 91501-970, Porto Alegre, RS, Brazil*

CONTENTS

I. INTRODUCTION

Water appears to be unique relative to other fluids in nature because of its several anomalous structural, thermodynamic, and dynamic properties.

The most familiar anomaly is its increasing density with temperature, at ambient pressure, up to 4°C. Above this temperature water behaves as a normal liquid and density decreases as temperature increases. Experiments for water allow to locate the line of temperatures of maximum density (TMD) in the pressure–temperature plane. Below TMD density decreases with decreasing temperature, differently

Liquid Polymorphism: Advances in Chemical Physics, Volume 152, First Edition.
Edited by H. Eugene Stanley.

from the behavior of the majority of fluids, for which density increases on lowering temperature [1].

Besides, a number of thermodynamic and dynamic anomalies water exhibit many solid phases due to structural and symmetry changes. Several coexistence lines separate the multiple solid phases. Thus, the energy landscape associated to the crystalline phases presents a number of sharp valleys with very low energies. The temperature and pressure ranges at which each one of these sharp valleys displays the lowest energy values define the stable phase in that region of the phase diagram. Those valleys of the energy landscape that never achieve the lowest energy correspond to the amorphous configurations. Therefore, it is reasonable to think that multiple amorphous phases are present. Even though the existence of water amorphous phases has been known since 1935 [2], the identification of two amorphous phases, one of lower density (LDA), the other of higher density (HDA)[3,4], as well as the suggestion of the existence of a very high-density amorphous phase (VHDA) [5], is quite recent.

Polyamorphism has been promoted as a means for understanding the anomalous thermodynamics and dynamics of water. It has been proposed that the increase of compressibility with the decrease of temperature is related to a second critical point at the end of a coexistence line between two liquid phases, a low-density liquid (LDL) and a high-density liquid (HDL) [6]. This critical point would be located in the supercooled experimentally inaccessible region [7–9]. In contrast, it is possible to explain the existing anomalies without invoking the presence of a critical point [9–11] and support the presence of a second critical without the need of polyamorphism [12].

Water, however, is not an isolated case. There are also other examples of tetrahedrally bonded molecular liquids such as phosphorus [13,14] and amorphous silica [15] that are other good candidates for having two liquid phases. Moreover, other materials such as liquid metals [16], graphite [17], and yttrium oxide-aluminum oxide [18] also exhibit thermodynamic anomalies.

What kind of potential would be appropriate for the description of tetrahedrally bonded molecular liquids in order to yield thermodynamic anomalies? Realistic simulations of water [19–21] have achieved a good accuracy in describing both thermodynamic and dynamic anomalies. However, due to the high number of microscopic details taken into account in these models, it becomes difficult to discriminate what are the essential ingredients to produce the anomalies. On the other extreme, a number of minimalistic isotropic models were proposed as the simplest framework capable of probing the physics of liquid–liquid phase transitions and liquid state anomalies. The desire to construct a simple two-body isotropic potential capable of describing water-like behavior has led to the design of a number of models in which single component systems of particles interact via core-softened (CS) potentials. Such model interactions present a repulsive core that exhibits a region of softening where the slope changes dramatically. This region can be a

shoulder or a ramp [22–37]. These two length scale models reproduce the density and diffusion anomalies, many solid phases and a reentrant spinodal. With the addition of an attractive interaction, these potentials also display a liquid–liquid transition besides liquid–gas coexistence. In this case, polymorphism arises due to the two arrangements allowed for by the two length scales.

The models cited above illustrate that directionality is not a fundamental ingredient neither for the presence of anomalies, nor of liquid–liquid coexistence, or even of polyamorphism. However, water molecule interactions due to hydrogen bonds exhibit directionality. What are the consequences of eliminating directionality or of replacing its effects with effective isotropic interactions? Lattice models represent the simplest framework for introducing directional interactions in the search for an answer to this question.

In the next section, we review a number of lattice gas models for which the addition of directional interactions not only allows for polyamorphism and two liquid phases but also introduces the possibility of a richer phase diagram, in which a critical line following the liquid–liquid first-order phase transition substitutes the critical point. Even though not explored in the literature, this picture is not inconsistent with known experimental results for water and other tetrahedral liquids [38].

II. ASSOCIATING LATTICE GAS IN TWO AND THREE DIMENSIONS

The directionality present in the H-bonding of water molecules and in other tetrahedral liquids can be represented by models that associate a lattice gas with bond orientation . This is the case of the associating lattice gas model introduced by Henriques and Barbosa [39] that is presented in the following two- and three-dimensional versions.

Consider a two-dimensional triangular lattice where each site may be empty or full. Associate to each site two kinds of variables: an occupational variable, σ_i, and an orientational variable, τ_i^{ij}. The orientational state of particle i is defined by the configuration of its bonding and nonbonding arms, as illustrated in Fig. 1. We consider two possible values for the ij arm variables. Four among the six arms can make a bond, with $\tau_i^{ij} = 1$, while the remaining two are inert arms, with $\tau_i^{ij} = 0$. Thus, there are three possible orientational states per particle. An energy γ is attributed to each pair of occupied neighboring sites that form a hydrogen bond, while nonbonding pairs are attributed an energy of ϵ. The overall energy is given by:

$$E = \epsilon \sum_{(i,j)} \sigma_i \sigma_j + \gamma \sum_{(i,j)} \sigma_i \sigma_j \tau_i \tau_j \tag{1}$$

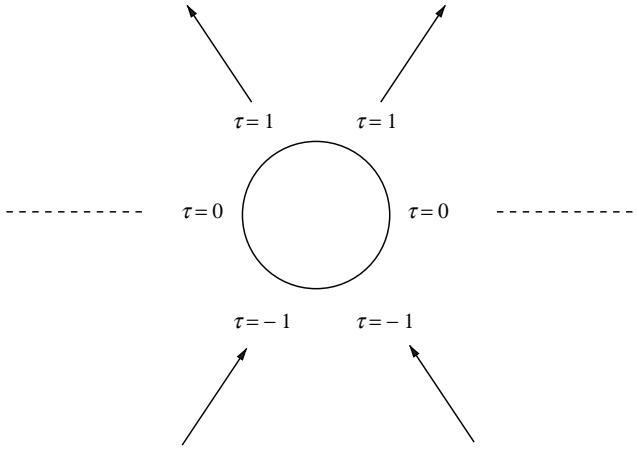

Figure 1. One possible orientational state for the molecule. Dashed lines correspond to non-bonding arms $\tau = 0$, whereas solid lines correspond to bonding arms $\tau = 1$ (donator) and $\tau = -1$ (acceptor).

where $\sigma_i = 0, 1$ are the occupational variables, $\tau_i^{i,j} = 0, \pm 1$ represents the arm states described above.

This system can exhibit a number of ordered states. In Fig. 2a, a system fully occupied with each molecule making four hydrogen bonds is shown. This is the ordered high-density phase (HD). Figure 2b illustrates the configuration in which the system has 3/4 of its sites occupied and each site has four hydrogen bonds. This is the ordered low-density phase (LD). The HD and LD energies per site are given by $e = 2\gamma + 3\epsilon$ and $e = 3(\epsilon + \gamma)/2$, respectively.

The zero temperature stable phases are obtained simply from comparison of the corresponding grand potentials per site. The latter are given, at zero temperature, by $\phi = e - \mu\rho$, where $\phi = \Phi/V$, $e = E/V$, N is the number of occupied sites and $\rho = N/V$ is the density of the system. Thus, at high chemical potential, the lowest grand potential per site is the one of the high-density phase ($\rho = 1$), as illustrated in Fig. 2, $\phi_{hdl} = 2\gamma + 3\epsilon - \mu$. As the chemical potential is decreased, the low-density phase ($\rho = 0.75$) with the grand potential per site given by $\phi_{ldl} = 3(\gamma + \epsilon)/2 - 3\mu/4$ becomes energetically more favorable and $\mu_{\mathrm{HDL-LDL}} = 2\gamma + 6\epsilon$ represents the coexistence point between the HD and the LD phases. Similarly, the pressure of coexistence between the two phases at zero temperature is given by $p_{\mathrm{HDL-LDL}} = 3\epsilon$. If the chemical potential decreases even further the gas phase with $\phi_{\mathrm{gas}} = 0$ becomes energetically more favorable and coexistence between the LD and a gas phases occurs at $\mu_{\mathrm{LDL-gas}} = 2(\gamma + \epsilon)$ and $p_{\mathrm{LDL-gas}} = 0$.

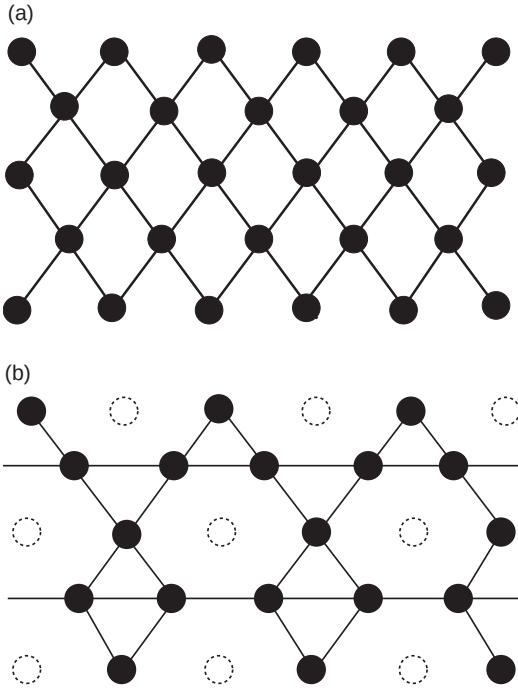

Figure 2. Representation of high-density liquid (HDL) (**a**) and low-density liquid (LDL) (**b**) phases. In the HDL phase, lattice is fully occupied and the nonbonding arms point to occupied sites. In the LDL phase three-fourth of the lattice is occupied and nonbonding arms point to empty sites.

Existence of an intermediate LD phase between the gas and the HD phases requires $p_{\mathrm{HDL-LDL}} > p_{\mathrm{LDL-gas}}$, which implies $\epsilon > 0$. Since ϵ represents the isotropic van der Waals-like interaction, the physical interpretation for this requirement is that ϵ represents an energetic penalty on pairs that do not form a bond.

For nonzero temperatures the complete $\overline{\mu} - \overline{T}$ phase-diagram obtained from numerical simulations for $\gamma = -2\epsilon$ is illustrated in Fig. 3 and goes as follows. At low-reduced chemical potentials, $\overline{\mu} = \mu/v$, for all reduced temperatures, $\overline{T} = T/v$, with $v = -\epsilon - \gamma$, only the gas phase is present. As the reduced chemical potential increases a low-density liquid phase (LDL) appears. This phase coexists with the gas phase along a first-order transition line at $\overline{\mu} = \overline{\mu}_{\mathrm{gas-LDL}}(\overline{T})$. For even higher reduced chemical potentials a high-density liquid phase (HDL) emerges. This phase coexists with the low-density liquid phase at the first-order line $\overline{\mu} = \overline{\mu}_{\mathrm{LDL-HDL}}(\overline{T})$.

Study of the system dynamics shows that at very low temperatures the diffusion coefficient in the high-density and low-density phases is zero, characterizing solid amorphous phases (LDA and HDA). Thus, starting from zero temperature at fixed chemical potential, the LDL and the HDL emerge continuously from the LDA

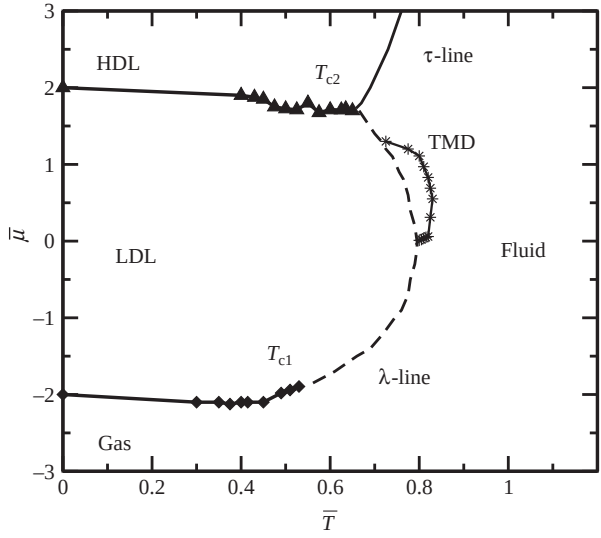

Figure 3. Chemical potential versus temperature phase diagram. Solid line and diamonds represent the Gas–LDL coexistence line, whereas solid line and triangles represent the LDL–HDL coexistence line. The temperature of maximum density (TMD) is represented by a solid line and stars. The dashed line is a critical line, named λ-line, and the solid line is another critical line named τ-line. λ-line emerges from the Gas–LDL coexistence line at a tricritical point T_{c_1} and meets the τ-line at the LDL–HDL coexistence line at a bicritical point T_{c_2}.

and the HDA phases, without any phase transition. The major difference between the LDL and the LDA phases is that in the first phase, the diffusion coefficient is nonzero while in the second the system does not diffuse. The same criteria apply for the HDL and HDA phases.

Such features of the statistical model resemble the low-density amorphous and high-density amorphous phases present in water. Similarly to what happens in water there is no phase transition but a continuous change form the amorphous to the supercooled liquid phases.

Finally, besides polyamorphism and liquid polymorphism, this model also exhibits density and diffusion anomalies [40,41].

A novel feature of this particular model relates to the terminus of the LDL–HDL coexistence line. The introduction of the orientational degrees of freedom through the τ variables leads to a richer phase diagram. The presence of an extra component, the orientation, in accordance with Gibbs' phase rule [42], gives rise to a critical line ending the coexistence between the two phases in place of the critical point presented by the isotropic soft-core models.

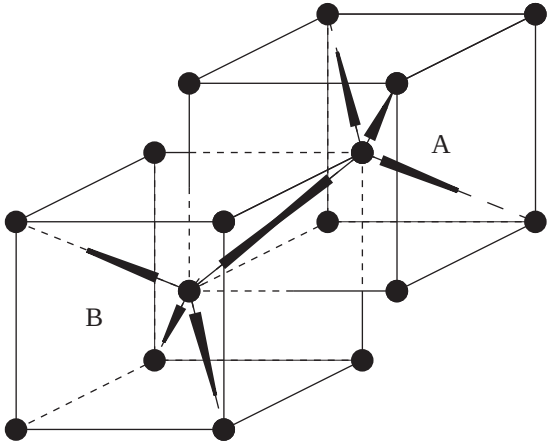

Figure 4. Two possible orientational states for a molecule, named A and B. Each particle has four-bonding arms with $\tau = 1$ and four-nonbonding arms with $\tau = 0$. Arms are distributed in a tetrahedral arrangement mimicking a real water molecule arrangement.

Now, let us consider the three-dimensional associating lattice gas model of $V = L^3$ sites on a body centered cubic (BCC) lattice, introduced by Girardi and coworkers[43] and described through a mean-field treatment by Buzano et al. [44]. The hamiltonian given by Eq. (1) is considered with the bonding and nonbonding arms distributed in a tetrahedral arrangement imposed by the lattice geometry. Four arms are the usual ice-bonding arms, while the remaining four arms are considered inert. Under these assumptions, each particle will found in one of two possible orientational states as illustrated in Fig. 4.

Similar to the two-dimensional case, at null temperature, a gas phase and two phases of different densities, LD and HD, may be present, depending on model parameters. The ordered high-density and low-density phases are represented in Fig. 5. As can be seen, in the LD phase only half the lattice is occupied and each particle bonds to all the four nearest neighbors, whereas in the HD phase all the sites are occupied and each molecule forms four bonds. At chemical potential $\mu_c = 2(\epsilon + \gamma)$, the gas phase ($\rho = 0$) coexists with the low-density (LD) phase with $\rho = 0.5$. The latter is present in the chemical potential range $2(\epsilon + \gamma) < \mu < 6\epsilon + 2\gamma$, yielding the condition that $\epsilon > 0$ for the existence of the LDL phase. At the chemical potential $\mu_c = 6\epsilon + 2\gamma$, the LD phase coexists with a high-density (HD) phase, with $\rho = 1$.

For nonzero temperatures, the model phase diagram given in terms of the reduced chemical potential, $\overline{\mu} = \mu/\epsilon$, versus reduced temperature , $\overline{T} = k_B T/\epsilon$, is illustrated in Fig. 6. Data are from numerical simulations for $\gamma = -2\epsilon$. As the temperature is increased the low- and high-density phases that may be identified as amorphous, due to a zero diffusion coefficient, smoothly turn into low- and high-density liquids, respectively, analogously to the two-dimensional case.

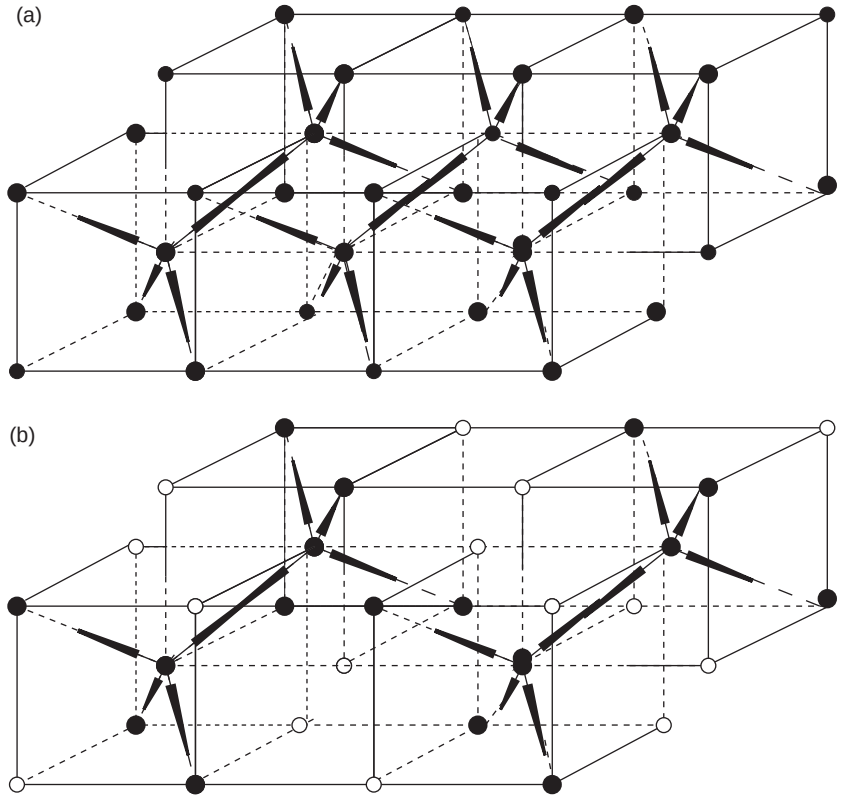

Figure 5. Representation of high density (HDL) (**a**) and low density (LDL) (**b**) phases. In the HDL phase, lattice is fully occupied and the nonbondig arms point to occupied sites. In the LDL phase, half of the lattice is occupied and nonbonding arms point to empty sites.

The coexistence between the LDL and the HDL phases ends at a tricritical point. The critical line emerging from this tricrical point, the λ line, is characterized by disordering of position distribution, described through sublattice densities, while the critical line at higher temperatures, the τ line, is characterized by orientational ordering on sublattices.

The three-dimensional model system also exhibits density and diffusion anomalous behavior [43,45].

In resume, introduction of the orientational degrees of freedom produce a critical line emerging from the coexistence between the two liquid phases for both the two-dimensional and the three-dimensional versions of the associating lattice gas.

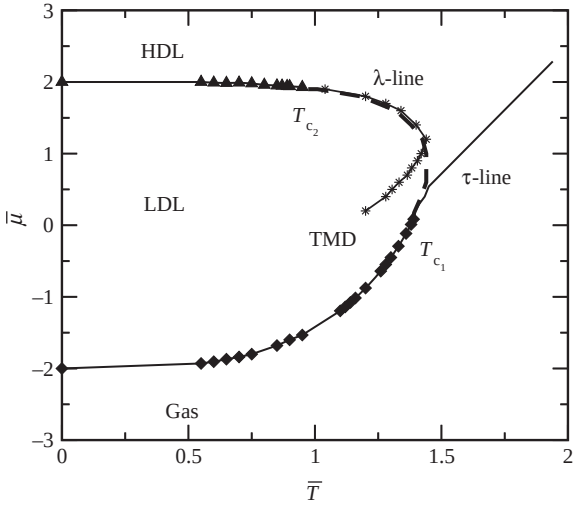

Figure 6. Chemical potential versus temperature phase diagram. Solid line and diamonds represent the Gas–LDL coexistence line whereas solid line and triangles represent the LDL–HDL coexistence line. The temperature of maximum density (TMD) is represented by a solid line and stars. The dashed line is a critical line, named λ-line, and the solid line is another critical line named τ-line. λ-line emerges from the LDL–HDL coexistence line at a tricritical point T_{c_2} and meets the τ-line at the Gas–LDL coexistence line at a bicritical point T_{c_1}.

III. BELL-LAVIS WATER MODEL

The Bell-Lavis model, introduced in the 1970's, and whose mean-field phase diagram was described recently [46], is a two-dimensional system in which molecules are located on a triangular lattice and are represented by two kinds of variable, σ and τ, in order to represent occupational and orientational states. Each molecule has six arms, separated by 120°, three of them inert, with $\tau_i^{ij} = 0$, while the other three are the bonding arms, with $\tau_i^{ij} = 1$. These conditions yield two possible orientations per particle, as illustrated in Fig. 7 . Examples of maximally bonded configurations of different densities are illustrated in Fig. 8.

Two neighbor molecules interact via van der Waals and hydrogen bonding of energies given, respectively, by parameters ϵ and $\epsilon + \gamma$. The model is described by the following effective Hamiltonian, in the grand-canonical ensemble:

$$\mathcal{H} = \sum_{(i,j)} \sigma_i \sigma_j (\gamma \tau_i^{ij} \tau_j^{ij} + \epsilon) - \mu \sum_i \sigma_i \tag{2}$$

where μ is the chemical potential.

A feature that distinguishes the Bell-Lavis model from the ALG models discussed in the previous section is that even the lowest energy configurations of the high-density phase ($\rho = 1$) involve frustration of the hydrogen bonds. As a consequence, the LD phase is present also for attractive van der Waals $\epsilon < 0$, in contrast with both versions of the ALG.

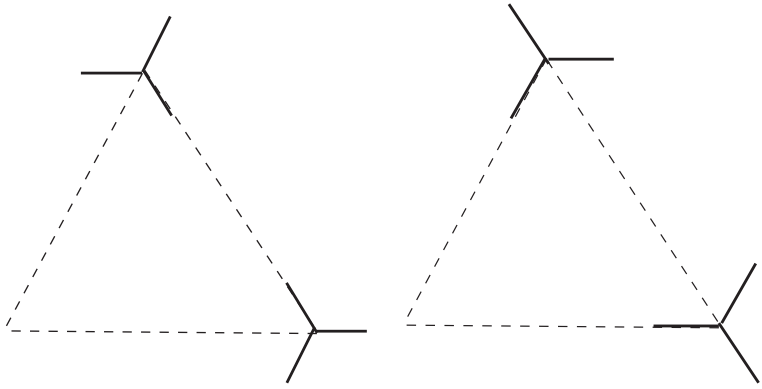

Figure 7. Bell-Lavis water model interactions. Two orientations of the water particles.

At zero temperature, a gas phase coexists with a low density phase at lower chemical potential, while a low-density phase coexists with a high-density phase at higher chemical potential.

As the temperature is increased, the low-density and the high-density phases turn continuously into the low-density liquid (LDL) and the high-density liquid (HDL) phases, respectively, as identified from the smooth emergence of nonzero diffusion coefficients [47,48].

Chemical potential $\overline{\mu} = \mu/-\epsilon$ versus temperature $\overline{T} = k_{\mathrm{B}}T/-\epsilon$ phase diagrams are shown in Fig. 9a, b, for two different ratios of van der Waals to bonding

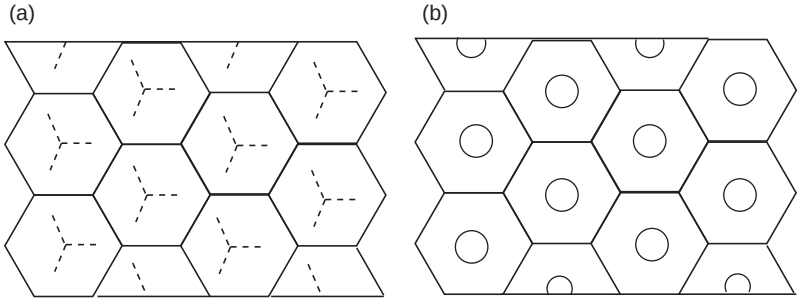

Figure 8. Representation of high-density (HDL) (**a**) and low-density (LDL) (**b**) liquid phases for the model. In the HDL phase, the lattice is fully occupied whereas in the LDL phase lattice is two-third occupied and nonbonding arms point to empty sites, forming a honeycomb structure.

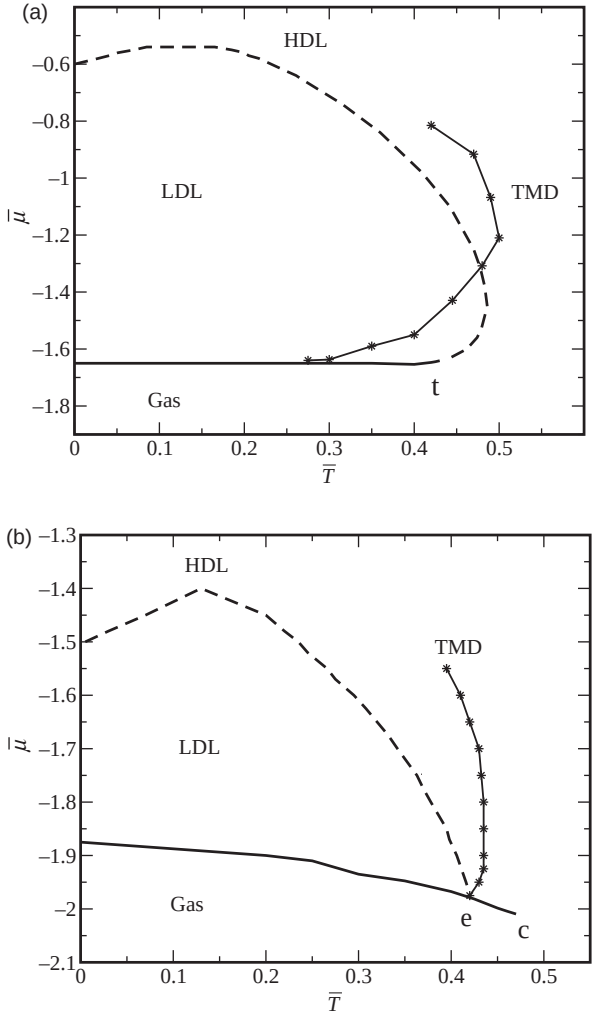

Figure 9. (**a**) Chemical potential versus temperature phase diagram for $\zeta = 1/10$. (**b**) Chemical potential versus temperature phase diagram for $\zeta = 1/4$. In both phase diagrams, solid line represents the Gas–LDL coexistence line, dashed line represents the LDL–HDL critical line, and solid line with stars, represents the TMD. In the $\zeta = 1/10$ case, coexistence line ends in a tricritical point t , while in the $\zeta = 1/4$ case, coexistence line ends in a critical point c. The critical line meets the coexistence line in a critical end point e.

energies, $\gamma = 9\epsilon$ and $\gamma = 3\epsilon$, respectively. The phases of different density are separated by a critical line, shown in the figure, in which data are from Monte Carlo simulations. Differently from the previous models, HD–LD coexistence is present for negative values of the van der Waals parameter ϵ, but only at null temperature ($T = 0$). The order parameter associated to the critical line in the Bell model is orientational sublattice density.

The Bell–Lavis model also presents density and diffusion anomalous behavior [47,48].

IV. CONCLUSIONS

Here we have explored two lattice orientational models (one of them in two and three dimensions) that exhibit two low-temperature amorphous-like phases that become liquid as the temperature is increased. Differently from isotropic continuous models, the orientational models that we have investigated present bicritical or tricritical points at the terminus of the liquid–liquid coexistence line. This higher order criticality is due to the introduction of an additional number of degrees of freedom in the system and is consistent with the Gibbs phase rule [42].

The Gibbs phase rule describes the possible number of degrees of freedom (f) in a closed system at equilibrium, in terms of the maximum number of stable phases (M) and the number of system components (N) as $f = N - M + 2$. The number of degrees of freedom for a system at equilibrium is the number of intensive variables (often taken as the pressure, temperature, composition fraction, or orientations) that may be arbitrarily specified without changing the number of phases. In a region with M stable phases, the values of the $N - M + 2$ state variables can be changed independently while preserving the same set of stable phases.

In the lattice models studied here, there are two system components: density and orientation with the corresponding conjugate fields, chemical potential μ and some "staggered" orientational field λ. This implies that liquid–liquid coexistence must be represented by a plane in (T, μ, λ) space, with $f = 2$. Our phase diagrams are sections of this plane, in which HD–LD coexistence appears as a line. Accordingly this coexistence plane may be limited by critical surfaces, as in the case of the associating lattice gas in two dimensions, or by a critical line, as in the three-dimensional associating lattice gas model or in the Bell-Lavis water models. Both cases are consistent with the Gibbs phase rule.

As for real water, it is not clear if the orientation imposed by hydrogen bonding is so relevant as to actually lead to a critical line instead of a critical point at the end of the hypothetic two liquid phase coexistence. However, this picture can not be excluded. The peaks in the specific heat observed in the confined water system could be an indication of criticality, indication that would only be confirmed if experiments in bulk water would be possible [38].

REFERENCES

1. C. A. Angell, E. D. Finch, and P. Bach, *J. Chem. Phys.* **65**, 3065 (1976).
2. E. F. Burton and W. F. Oliver, *Proc. R. Soc. Lond. A* **153**, 166 (1935).
3. O. Mishima, L. D. Calvert, and E. Whalley, *Nature* **310**, 393 (1984).
4. O. Mishima and H. E. Stanley, *Nature* **396**, 329 (1998).
5. R. Martonak, D. Donadio, and M. Parrinello, *Phys. Rev. Lett.* **92**, 225702 (2004).
6. P. H. Poole, F. Sciortino, U. Essmann, and H. E. Stanley, *Nature* **360**, 324 (1992).

7. F. W. Starr, F. Sciortino, and H. E. Stanley, *Phys. Rev. E* **60**, 6757 (1999).
8. F. W. Starr, S. T. Harrington, and H. E. Stanley, *Phys. Rev. Lett.* **82**, 3629 (1999).
9. P. Debenedetti, *J. Phys.: Condens. Matter* **15**, R1669 (2003).
10. S. Sastry, P. G. Debenedetti, F. Sciortino, and H. E. Stanley, *Phys. Rev. E* **53**, 6144 (1996).
11. G. N. I. Clark, G. L. Hura, J. Teixeira, A. K. Soper, and T. Head-Gordon, *PNAS* **107**, 4003 (2010).
12. Y. Liu, A. Z. Panagiotopoulos, and P. G. Debendedetti, *J. Chem. Phys.* **131**, 104508 (2009).
13. Y. Katayama, T. Mizutani, W. Utsumi, O. Shimomura, M. Yamakata, and K. Funakoshi, *Nature* **403**, 170 (2000).
14. G. Monaco, F. S., W. A. Crichton, and M. Mezouar, *Phys. Rev. Lett.* **90**, 255701 (2003).
15. D. J. Lacks, *Phys. Rev. Lett.* **84**, 4629 (2000).
16. P. T. Cummings and G. Stell, *Mol. Phys.* **43**, 1267 (1981).
17. M. Togaya, *Phys. Rev. Lett.* **79**, 2474 (1997).
18. G. N. Greaves, M. C. Wilding, S. Fearn, F. Kargl, L. Hennet, W. Bras, O. Jajérus, and C. M. Martin, *J. Non-Cryst. Sol.* **355**, 715 (2009).
19. F. H. Stillinger and A. Rahman, *J. Chem. Phys.* **60**, 1545 (1974).
20. H. J. C. Berendsen, J. R. Grigera, and T. P. Staatsma, *J. Chem. Phys.* **91**, 6269 (1987).
21. M. W. Mahoney and W. L. Jorgensen, *J. Chem. Phys.* **112**, 8910 (2000).
22. E. A. Jagla, *Phys. Rev. E* **58**, 1478 (1998).
23. E. A. Jagla, *J. Chem. Phys.* **110**, 451 (1999).
24. M. R. Sadr-Lahijany, A. Scala, S. V. Buldyrev, and H. E. Stanley, *Phys. Rev. Lett.* **81**, 4895 (1998).
25. M. R. Sadr-Lahijany, A. Scala, S. V. Buldyrev, and H. E. Stanley, *Phys. Rev. E* **60**, 6714 (1999).
26. P. A. Netz, S. Buldyrev, M. C. Barbosa, and H. E. Stanley, *Phys. Rev. E* **73**, 061504 (2006).
27. A. B. de Oliveira, P. A. Netz, T. Colla, and M. C. Barbosa, *J. Chem. Phys.* **124**, 084505 (2006).
28. A. B. de Oliveira, P. A. Netz, T. Colla, and M. C. Barbosa, *J. Chem. Phys.* **125**, 124503 (2006).
29. A. B. de Oliveira, P. A. Netz, and M. C. Barbosa, *Eur. Phys. Jour. B* (2008).
30. A. B. de Oliveira, G. Franzese, P. A. Netz, and M. C. Barbosa, *J. Chem. Phys.* **128**, 064901 (2008).
31. A. B. de Oliveira, E. B. Neves, C. Gavazzoni, J. Z. Paukowski, P. E. Netz, and M. C. Barbosa, *J. Chem. Phys.* **8132**, 164505 (2010).
32. N. B. Wilding and J. E. Magee, *Phys. Rev. E* **66**, 031509 (2002).
33. R. Kurita and H. Tanaka, *Science* **206**, 845 (2004).
34. P. J. Camp, *Phys. Rev. E* **68**, 061506 (2003).
35. P. J. Camp, *Phys. Rev. E* **71**, 031507 (2005).
36. Y. D. Fomin, N. V. Gribova, V. N. Ryzhov, S. M. Stishov, and D. Frenkel, *J. Chem. Phys.* **129**, 064512 (2008).
37. V. N. Ryzhov and S. M. Stishov, *Phys. Rev. E* **67**, 010201 (2003).
38. H. W. Sheng, H. Z. Liu, Y. Q. Cheng, J. Wen, P. L. Lee, W. K. Luo, S. D. Shastri, and E. Ma, *Nature Mater.* **6**, 192 (2007).
39. V. B. Henriques and M. C. Barbosa, *Phys. Rev. E* **71**, 031504 (2005).
40. M. M. Szortyka, M. Girardi, V. B. Henriques, and M. C. Barbosa, *J. Chem. Phys.* **130**, 184902 (2009).
41. M. M. Szortyka and M. C. Barbosa, *Physica A* **380**, 27 (2007).
42. H. B. Callen, *Thermodynamics and an Introduction to Thermostatistics*, John Wiley, New York, 2nd ed., 1960.

43. M. Girardi, M. M. Szortyka, V. B. Henriques, and M. C. Barbosa, *Physica A* **386**, 692 (2007).
44. C. Buzano, E. De Stefanis, and M. Pretti, *J. Chem. Phys.* **129**, 024506 (2008).
45. M. M. Szortyka, M. Girardi, V. B. Henriques, and M. C. Barbosa, *J. Chem. Phys.* **132**, 134904 (2010).
46. M. A. A. Barbosa and V. B. Henriques, *Phys. Rev. E* **77**, 051204 (2008).
47. C. E. Fiore, M. M. Szortyka, M. C. Barbosa, and V. B. Henriques, *J. Chem. Phys.* **131**, 164506 (2009).
48. M. M. Szortyka, C. E. Fiore, V. B. Henriques, and M. C. Barbosa, *J. Chem. Phys.* **133**, 104904 (2010).